A POLYNOMIAL DIFFERENTIAL QUADRATURE-BASED NUMERICAL SCHEME TO SIMULATE THE NERVE PULSE PROPAGATION IN THE SPATIAL FITZHUGH-NAGUMO MODEL

CAGLAR UYULAN[*]

Department of Mechatronics Engineering, Bülent Ecevit University, Zonguldak, Turkey

Abstract: Nonlinear dynamics connect the neurons that form the brain, and thus, the complex information is produced and transported. The function of the neurons and the problem of understanding the dynamics of the brain has been the research area of mathematical neuroscience. In this study, the modelling and simulation of the propagation of the electric field based Action Potential (AP) on the Two Dimensional (2-D) field of axon network, whose matrix consists of 128×128 electrically coupled neurons were done using nonlinear Spatial FitzHugh Nagumo (SFN) equations. SFN equations are a particular class of Partial Differential Equation's (PDE's) exhibiting travelling wave behaviour occurred in neuron systems. The motivation of this paper is to evaluate the SFN equation, which is a special kind of the time-dependent nonlinear reaction-diffusion problem governing neuron dynamics numerically in 2-D space addressed by investigating the Polynomial-based Differential Quadrature Method (PDQM) having Chebyshev-Gauss-Lobatto quadrature points. The solution occurs as elliptical spiral waves induced by electrical stimulation. Thus, the neuronal system behaviour and the interaction with the specific type of Boundary Conditions (BC's) are predicted. The space derivatives are discretised through PDQM. In this way, the problem is reduced into a system of first-order

[*]Corresponding author

E-mail address: caglaruyulan@beun.edu.tr

non-linear differential equations. Hereafter the time derivatives of the SFN equation are solved through the Finite Difference Method (FDM). The various dynamical behaviour that governs the travelling wave pattern regarding the Initial Condition's (IC's), BC's and way of stimulation of the neuron model examined in details. Numerical results indicated that the proposed PDQM provide reliable, fast, and efficient solutions.

Keywords: numerical analysis; polynomial differential quadrature method; neuron modelling; travelling wave; time-dependent nonlinear reaction-diffusion equation; brain dynamics; FitzHugh-Nagumo equation.

2010 AMS Subject Classification: 65Z05, 65P99, 92B20.

1. INTRODUCTION

SFN equation is a type of nonlinear reaction-diffusion equation, which takes place in scientific models covering fluid mechanics, plasma physics, computational neuroscience, chemical kinematics etc. [1-4]. The reaction-diffusion mechanism expresses itself as a form of a travelling wave propagating in a medium. Travelling waves, which associated with having a constant velocity along with its propagation process move in a particular direction by maintaining a specific pattern. The impulses occurred in the multidimensional nerve fibre arrays are described as travelling wave propagation in mathematical neurophysiology [5]. It is essential to determine the stability for perturbations in the IC's for solutions of the full PDE [6].

The travelling wave solutions defined as $v(x,t) = V(z)$, where $z = x - ct$. The spatial and time domains correspond to the $"x"$ and $"t"$ notations, respectively. The velocity of the wave is expressed as $"c"$. The exact analytical solution of SFN-type equation is sought-after. Therefore it is necessitated to be used numerical methods to approximate exact solutions. Information transmission is realised through AP mechanism following a consistent trajectory in the nerve cell membrane. The proteins which take place in the membrane are responsible for the AP allowing specific ions to pass through various conformations of voltage-gated ion channels. The polarised membrane collects the depolarizing stimulus from dendrites, and the AP advances along the axon reconciled by the ion-channels spreading along with it.

In the *depolarisation* phase, Na^+ channels, which allow the Na^+ Ions to enter the neuron, are

opened at the resting membrane when exposed to a stimulant. The increase in the positive ions within the cell depolarises the membrane potential and provides it to reach the threshold potential. Therefore, more Na^+ channels are opened, and the voltage in the membrane is reversed rapidly and reaches its most positive value.

At the peak of the AP, many of the voltage-gated Na^+ channels begin to close and several positive K^+ Channels open at the same time allowing positive charges to separate from the membrane. This action, called a *"re-polarisation"* phase, causes the membrane potential to return to resting state. Then the membrane re-polarises beyond the resting state as a result of more open K^+ Channels. The return to steady-state continues as the K^+ Channels close. This phase is known as the *refractory period* or *hyper-polarisation* phase. The electrical signal is transformed into a chemical signal at the synapse [7].

Hodgkin and Huxley investigated the neural excitability through voltage-clamp experiments and characterised the properties of ionic conductances and membrane potential, which originate AP. Stepwise depolarisation of the membrane was realised in these experiments through the help of the electrodes. The inward and outward current was triggered, respectively. In this way, the net current could be dichotomised into fast inward component transported by Na^+ ions, and slow outward component carried by K^+ Ions. These two kinds of currents are caused by independent permeability mechanisms for Na^+ and K^+, which contain the voltage-induced conductors of a particular object in the membrane [8]. The most important achievement of this theory was that the experimental voltage-clamp data consistently coincided with a quantitative model for excitability of a nerve pulse. The shape and propagation of the AP, threshold, and refractory period can be generated from the Hodgkin-Huxley (HH) model. However, there exists a complexity because the values of the conductances are dependent on the empirical functions of voltage and time. HH model relates the ion channels to the currents and APs. Due to the outnumbered differential equations describing the model, the computational burden of the simulation is very high. HH dynamics are reduced to 1-D or 2-D systems, which are practical for mathematical analysis utilising phase-portraits and reveal the neuronal behaviour. However, these systems are parameter-

sensitive. The parameters should be measured for various neurons and be used statistical tools to capture optimal conditions. The reliability of the model is low because it is not sustainable to estimate parameters for a specific neuron having a conductivity-based model. It is not possible to produce a general model to mimic all neurobiological features of a neuron. Therefore, various models are commonly derived to simulate neuronal networks and to rationalise the experimental data. These models are SFN, Hindmarsh-Rose, Morris-Leccar, Rajagopal, respectively [9].

Waves of electrical and neuromuscular excitability were sought in various physiological subjects such as temporally periodic and spatially distributed contractions of atria and ventricles [10], and waves of diffusion in the cerebral cortex and retina [11, 12]. Travelling waves regarding reaction-diffusion kinetics are observed and analysed for two-and three-spatial dimensions [13-20].

To understand spiral wave dynamics, it is essential to investigate the excitability of the nerve cells, cardiac tissue etc. Computer simulations, which are capable of solving partial differential equations related to physiological reaction-diffusion kinetics, serve an excellent service to comprehend this issue and to exploit with the results acquired through experiments. Therefore it necessitates developing efficient and reliable numerical methods to solve this kind of reaction-diffusion equations.

The research presented in the literature is based on the building of fast and accurate numerical schemes to simulate models for wave propagation, spiral wave occurrence, and to clarify the process of initiation, reflection and disintegration of a spiral wave, and to predict how the spiral wave behaves with BC's [21-24]. The theoretically based analysis for travelling wave solutions of a nerve conduction equation was analysed regarding periodic solutions, propagation speeds and stability, which validates conjecture made before for other nerve conduction equations [25]. A novel approach for solving the generalised SFN equation with time-dependent parameters was implemented [26].

Exact travelling wave solutions were found comprising periodic function solutions, soliton-like solutions, and trigonometric function solutions, respectively. A $2-D$ fractional SFN monodomain model on an irregular domain, which consists of a coupled Riesz space fractional

nonlinear reaction-diffusion model was investigated by developing a novel spatially second-order accurate semi-implicit alternating direction method. The stability and convergence of this method were proved, and numerical examples were solved to aid theoretical analysis. Such model demonstrates a robust modelling approach for understanding various aspects of electrophysiological behaviour in biological tissue [27]. The existence and exponential stability of travelling wave solutions of some integro-differential equations emerging from neuronal networks were concerned via fixed point theorems, and the exponential stability of waves was investigated through linearization technique [28]. Two cases comprising various types of uniform steady-state distributions for the initiation of propagating front solution was investigated to analyse the conditions for a propagating wave in the Nagumo-type discrete reaction-diffusion model [29].

In this paper, the PDQM method was selected to solve the problem above. DQM is a numerical approach for solving initial and boundary value problems. This method has been developed as an alternative solution procedure for finite difference and finite element techniques. The DQM, which is inspired by the conventional integral quadrature method, converges to the partial derivative of a function regarding a coordinate located at any point by a linear weighted sum of all functional values lied on a mesh (grid) line.

Determination of weighting coefficients is the essential step in the DQM application [30]. The methods presented in the literature to evaluate the weighting coefficients comprise algebraic formulation whose coordinates of grid points are selected as the roots of the Legendre Polynomials, explicit formulations acquired through Lagrange Interpolated polynomials, and analysis of a high order polynomial approximation and linear vector space [31]. The accuracy and minimal computational effort of the DQM has been proved thoroughly with a many application in applied mathematics, physics and engineering especially in computational biology, fluid mechanics, structural mechanics, aeroelasticity etc [32].

A broad spectrum of problems containing deflection, buckling, and the natural frequency of flexible beams and plates, including various clamped, free and supported types were investigated through DQM [33-36]. Based on these numerical solutions, it can be concluded that the DQM

yields excellent accuracy as compared to the analytical solutions even if a small number of grid points is utilised. The accuracy of the DQM method was also tested by applying it to the buckling analysis of the thin and isotropic plates whose shapes are rectangular, circular, square, skew, trapezoidal, annular, and sectorial subjected to different BC's. The generalised DQM was introduced to overcome the possible singularity problem of the original one in acquiring the weighting coefficients and solving for natural frequencies of some structures under various BC's. Generalised DQ-based vibration analysis of beams and plates was investigated to eliminate the adverse effects of the δ −technique, which discretises the derivative BC's at a point of distance δ away from the boundary. It can be deduced that the presented approach suits well for any combination of supported and clamped BC's [37]. DQ solution of the higher-order differential equation, which comprise the implementation of the multiple BC's has been accurately applied to the problem of the free vibration of plates [38].

Theoretical calculations such as the relationship among the DQM and the conventional discretisation techniques, error analysis, and the effect of grid point distributions on stability and accuracy have been conducted with the explicit calculation of weight coefficients and their application in various fields [39, 40]. The DQM was extended for the evaluation of 2-D PDE's to cover problems with arbitrary geometry and was verified with the results of thermal and torsional problems [41]. Irregular elements of the DQM were applied to the steady-state heat conduction problem using mapping-based transformation technique, which converts the natural transition condition of two adjacent elements and Neumann BC's designated on the variable physical element into parent space [42]. A locally one-dimensional time integration scheme for the diffusion equation in 2-D space was defined based on the extended trapezoidal formula to suppress unwanted vibrations in the solution [43]. Time-dependent diffusion problem was investigated with a hybrid numerical scheme whose time derivative was discretised by utilising DQM, and spatial partial derivatives were discretised by using a dual reciprocity boundary element method [44]. In [45], a paired pseudospectral DQM was proposed to solve a class of hyperbolic multidimensional telegram equation. The theoretical analysis and numerical tests indicated that this method exhibits

spectral-sensitive convergence in the spatial area and has stability in the time domain.

In this paper, PDQM is applied to SFN, which is a particular case of a time-dependent nonlinear reaction-diffusion problem that occurred in neuron array, in 2-D space to discretise the space variables. The time derivatives of the equation system are discretised through FDM for sustaining broader stability region. Time-dependent BC's are discussed. Stability criteria are also controlled via various values of time increment Δt and some grid points N in a space region. It was focused on the SFN model because this model serves an elegant qualitative description of the HH model, providing a better understanding of the qualitative dynamical behaviour of the neuron. HH model has four main dynamics, which represents fast and slow kinetics. While membrane potential and Na^+ activation channel changes quickly, K^+ activation channel and Na^+ Inactivation channel varies slowly. In the SFN model, slow variables are fixed, and fast variables are considered. These variables are suitable for investigating the excitability, bursting and wave propagation. The propagation pulse is derived from cable theory expressing the inward and outward (radial) currents, which are caused by voltage-gated ion channels, for any arbitrary point along the axon. The BC's was applied periodically at the edge of the element and along the continuum boundary. Two different stimulus method was utilised to initiate various spiral wave solutions in the simulation. The detailed analysis and discussions were done. The primary motivation of this paper is to contribute predictive neural modelling problem encountered in the computational neuroscience.

2. THEORETICAL BACKGROUND

2.1. Spatial FitzHugh-Nagumo Equation

The SFN equations have been sought genuinely to model electrical activity in neuron cells as a simplification of the HH model. The SFN model given in Eq.1 describes the impulse transportation phenomena as a reaction-diffusion kinetic along with the neuron cells, which takes into account the effects of memory bounded through the presence of the internal structure [46].

$$\frac{\partial v(x,y,t)}{\partial t} = G_x * \frac{\partial^2 v(x,y,t)}{\partial x^2} + G_y * \frac{\partial^2 v(x,y,t)}{\partial y^2} - c_1 * f\big(v(x,y,t)\big) - c_2 * r(x,y,t) * v(x,y,t) + I(x,y,t)$$

$$\frac{\partial r(x,y,t)}{\partial t} = b * v(x,y,t) - \gamma * r(x,y,t) \qquad (x,y) \in \Omega, [N, M] \quad t \in [0,T] \qquad (1)$$

where $f\big(v(x,y,t)\big) = v(x,y,t) * \big(a - v(x,y,t)\big) * (1 - v(x,y,t))$; a, b and γ are positive

constants. a is the excitation threshold, b, c_1, c_2, and γ are the parameters related to the

resting state and dynamics of the system, respectively. G_x and G_y are the parameters related to

the diffusion coefficient, respectively. $I(x,y,t)$ is the driving stimulus of the external current.

Eq.1 subject to mixed Dirichlet and Neumann BC's, respectively and various spatial and timing

pattern of the applied external stimulus is solved by using a PDQM-FDM hybrid numerical scheme.

Subject to Dirichlet BC's

$$v(0,y,t) = 0, v(N,y,t) = g_1(t) \quad , \quad v(x,0,t) = 0, v(x,M,t) = g_2(t) \qquad , \qquad t \in [0,T]$$

where $g_1(t) = \frac{1}{2} + \frac{1}{2}\tanh\left(\frac{1}{2\sqrt{2}}\left(N - \frac{2a-1}{\sqrt{2}}t\right)\right)$ $\qquad g_2(t) = \frac{1}{2} + \frac{1}{2}\tanh\left(\frac{1}{2\sqrt{2}}\left(M - \frac{2a-1}{\sqrt{2}}t\right)\right)$

Subject to Neumann BC's

$$\frac{\partial v(0,y,t)}{\partial x} = 0, \quad \frac{\partial v(N,y,t)}{\partial x} = g_3(t), \qquad\qquad t \geq 0$$

$$\frac{\partial v(x,0,t)}{\partial y} = 0, \quad \frac{\partial v(x,M,t)}{\partial y} = g_4(t), \qquad\qquad t \geq 0$$

where $g_3(t) = \frac{1}{2} + \frac{1}{2}\tanh\left(\frac{1}{2\sqrt{2}}\left(N - \frac{2a-1}{\sqrt{2}}t\right)\right)$ $\qquad g_4(t) = \frac{1}{2} + \frac{1}{2}\tanh\left(\frac{1}{2\sqrt{2}}\left(M - \frac{2a-1}{\sqrt{2}}t\right)\right)$

Subject to the IC

$$v(x,y,0) = \hat{h}(x,y), 0 \leq x \leq N, 0 \leq y \leq M$$

where $\hat{h}(x,y) = [\frac{1}{2} + \frac{1}{2}\tanh\left(\frac{x}{2\sqrt{2}}\right), \frac{1}{2} + \frac{1}{2}\tanh\left(\frac{y}{2\sqrt{2}}\right)]$

where (x,y) represents the spatial coordinates, and t indicates the time.

The variables $v(x,y,t)$ moreover, $r(x,y,t)$ are the membrane voltage and the recovery

variables at position x, y and time t, respectively. $x\ and\ y$ correspond to the position of the

neurons in $2 - dimensional\ array$. $v(x,y,t)$ describes the voltage spreading along the

cylindrical membrane as a function of distance x, y and time t. The BC's and IC must be

determined. The model is capable of catching the spiral waves in 2-D as well as other phenomena

in $3 - D$. The system of equation in Eq.1 is utilised for the qualitative study of a nerve axon pulses,

as well as for the description of general excitable media. Generated travelling waves represent a

diffusion term as the second derivative in spatial coordinates. In this way, the stimulated AP along the axon is simulated in the cortical neural network in the form of the propagation of electrical potential waves.

The main difficulty to find the exact analytical solution of the SFN model is the nonlinear function $f\big(v(x,y,t)\big)$. The existence and uniqueness of a travelling wavefront solution have been proved and, the stability of the travelling wave solution for a general class of initial data including nerve axon impulse creation and propagation and other patterns in dissipative systems has been described [47].

Whenever solving the PDE given in Eq.1, there might be encountered various errors, such as truncation, roundoff, stability errors [48]. The SFN equation system has a unique attractor with two modes of turning back to a resting state. Under a small amplitude excitation, the system represents a short recursion in phase space before reaching equilibrium. When a large amplitude excitation is performed, the method follows a longer path in phase space before retaining to balance.

2.2. Polynomial-based Differential Quadrature Method

DQM is based on linear vector space analysis and function approach. In PDQM, the solution of the ordinary differential equation is approached with a high degree of a polynomial through which the weight coefficients of the polynomial are determined. The polynomial can be stated with the specified weight coefficients, and a solution polynomial, which is closer to the solution of the ODE is obtained. The weight coefficients for PDQM were first calculated by Bellman and Casti [40]. The grid points in this formula are selected from the roots of the translated Legendre polynomial. However, as the number of grid points growths, the number of an equation in the algebraic equation system increases. Therefore, the coefficient matrix will not be able to give a precise result. Accordingly, it is challenging to determine the weight coefficients when the number of grid points is high. The Lagrange interpolation polynomial was taken by Quan and Chang to evaluate the weight coefficients for the first and second-order derivatives. Shu and Richards have proved that all approaches calculate weight coefficients in PDQM can be formed from the choice of base vectors in the linear vector space [49, 50]. The weight coefficients calculated in these various

methods ultimately yield the same values. This idea has been introduced by utilising the linear vector space properties. Shu has developed an algebraic recurrence formula for evaluating the weight coefficients of first and high-order derivatives. There are no restrictions on the selection of grid points in this formula.

Let us assume that $f(x)$ is a function and x_i is the grid points, which separates the area under $f(x)$. According to this assumption, the first-order derivative of the $f(x)$ function w.r.t x at x_i point approximates to the sum of the weighted linear function values at all values in the definition zone $[x_A = x_1, x_2, \ldots, x_M = x_B]$ given in Eq.2

$$\frac{d f(x_i)}{dx} = \sum_{j=1}^{M} \left(A_{ij} * f(x_j) \right), \quad i = 1, 2, \ldots, M \tag{2}$$

where A_{ij} is the weight coefficients and M is total grid point number.

A_{ij} weight coefficients take different values w.r.t x_i points. The main concern of the DQM is to define A_{ij} weight coefficients. Several approaches have been developed to determine these weight coefficients.

Let us assume that $f(x)$ is a function, and $r_k(x)$ is a base polynomial. Weight coefficients A_{ij} are evaluated using the equations presented in Eq.3, which can be deduced from Eq.2.

$$f(x) = \sum_{k=1}^{M} \left(c_k * r_k(x) \right) \quad , \quad \frac{d f(x)}{dx} = \sum_{k=1}^{M} \left(c_k * \frac{d r_k(x)}{dx} \right) \quad \rightarrow \quad \frac{d r_k(x_i)}{dx} = \sum_{j=1}^{M} \left(A_{ij} * r_k(x_j) \right)$$

$$\tag{3}$$

where c_k are constant.

In this paper, we will focus on Shu's approach in the selection of base polynomial to determine the weight coefficients.

The general approach of Shu was derived from Bellman's criteria. This approach includes all procedures, including Quan and Chang approach. The emergence of this approach stems from two main problems. The first is that Belmann's two methods used in the calculation of weight coefficients. The other is that these two approaches give the same result. If these two approaches can provide the same result, other criteria should be obtained to evaluate the weight coefficients. These approaches can be structured by linear vector space analysis and a change of base polynomial by utilising the polynomial method. The solution of the ODE can be approximated

with a high-order polynomial. Let us assume that the order of the approximation polynomial as $N - 1$. This approximation polynomial constitutes a linear vector space $\vec{V}_M$ comprising vector sum and scalar multiplication operators and can be expressed in various forms.

A base polynomial is defined as in Eq.4 [30].

$$r_k(x) = \frac{M(x)}{(x - x_k) * M^{(1)}(x_k)}, \quad k = 1, 2, \dots, M \tag{4}$$

where $M(x) = (x - x_1) * (x - x_2) * \dots * (x - x_M)$, $M^{(1)}(x_i) = \prod_{k=1, k \neq i}^{M} (x_i - x_k)$

For simplicity, $M(x)$ can be set as; $M(x) = N(x, x_k) * (x - x_k), k = 1, 2, \dots, M$

with $N(x_i, x_j) = M^{(1)}(x_i) * \delta_{ij}$, where δ_{ij} is the Kronecker operator.

The weight coefficients A_{ij} are computed by following algebraic formulations given in Eq.5

$$A_{ij} = \frac{1}{x_j - x_i} \prod_{k=1, k \neq i, j}^{M} \frac{x_i - x_k}{x_j - x_k}, \quad for \ j \neq i$$

$$A_{ii} = \sum_{k=1, k \neq i}^{M} \frac{1}{x_i - x_k} \tag{5}$$

The operators for the discretisation of higher-order derivatives through Shu's recurrence formulation [30] is given in Eq.6

$$f_x^{(m-1)}(x_i) = \sum_{j=1}^{M} \left(A_{ij}^{(m-1)} * f(x_j) \right)$$

$$f_x^{(m)}(x_i) = \sum_{j=1}^{M} \left(A_{ij}^{(m)} * f(x_j) \right) \qquad i = 1, 2, \dots, M \quad ; m = 2, 3, \dots, M-1 \tag{6}$$

where $f_x^{(m-1)}(x_i)$, $f_x^{(m)}(x_i)$ demonstrate $(m-1)th$ and $(m)th$ order derivatives of $f(x)$ w.r.t x at x_i. $A_{ij}^{(m-1)}$ and $A_{ij}^{(m)}$ are the weight coefficients related to $f_x^{(m-1)}(x_i)$ and $f_x^{(m)}(x_i)$.

The explicit formulations for $A_{ij}^{(m)}$ are derived from two sets of base polynomials given in Eq.7

$$A_{ij}^{(m-1)} = \frac{N^{(m-1)}(x_i, x_j)}{M^{(1)}(x_j)} \quad , \qquad A_{ij}^{(m)} = \frac{N^{(m)}(x_i, x_j)}{M^{(1)}(x_j)} \tag{7}$$

The recurrence formulation is obtained as in Eq.8

$$A_{ij}^{(m)} = m * \left(A_{ij} * A_{ii}^{(m-1)} - \frac{A_{ij}^{(m-1)}}{x_i - x_j} \right) \qquad for \quad i, j = 1, 2, \dots, M \ ; m = 2, 3, \dots, M - 1$$

$$\tag{8}$$

where A_{ij} is the weight coefficient of the first-order derivative. The formulation $A_{ii}^{(m)}$ can be stated as in Eq.9

$$A_{ii}^{(m)} = \frac{M^{(m+1)}(x_i)}{(m+1)*M^{(1)}(x_i)} \qquad \text{for } i, j = 1, 2, \ldots, M \text{ ; } m = 2, 3, \ldots, M - 1 \tag{9}$$

The Matlab formula of the procedure defined above is represented in APPENDIX-I.

3. NUMERICAL APPROACH

3.1. Description of the numerical scheme

Before solving the SFN equation numerically, one must derive a fundamental condition that causes a pulse wave behaviour related to the parameters of the equation. The form of the solution is sought as

$$v = v(z) = v(x - ct) \text{ and } r = r(z) = r(x - ct)$$

Then the solution forms are replaced into the SFN equations given in Eq.1 to obtain Eq.10

$$-c * v' = D * v'' + v * (v - a) * (1 - v) - r$$

$$-c * r' = b * v - \gamma * r \tag{10}$$

Let $y = v'$ and $y' = v''$. Eq. 10 can be expressed as in Eq.11

$$D * y' = -c * y - v * (v - a) * (1 - v) + r$$

$$v' = y$$

$$r' = \frac{\gamma}{c} * r - \frac{b}{c} * v \tag{11}$$

The critical points $[D * y' = 0, v' = 0, r' = 0]$ can be defined as in Eq.12

$$\left(0, v_k, \frac{b}{\gamma} * v_k\right), k = 1, 2, 3 \tag{12}$$

where $\gamma > 0$ and v_k are the roots of

$$v_k * \left[\frac{b}{\gamma} - (v_k - a) * (1 - v_k)\right] = 0$$

The system represented in Eq.11 has two complex roots exhibiting a pulse solution with BC's of $v(\pm\infty) = 0$. It is necessitated to have a homoclinic orbit around a critical point $[v, v'] = [0,0]$ in phase space. It can be obtained from Eq.12 as

$$v_k - (a + 1) * v_k + \left(a + \frac{b}{\gamma}\right) = 0 \quad \text{whose complex roots are;}$$

$$(a + 1)^2 - 4 * \left(a + \frac{b}{\gamma}\right) < 0$$

If the following condition is satisfied, a pulse wave solution can be obtained

$$(1 - a)^2 < 4 * \left(\frac{b}{\gamma}\right)$$

The 2-D domain is partitioned into x_i, y_j grid point $i = 1, 2, ..., N, \quad j = 1, 2, ..., M$. Then Eq.1 becomes as in Eq.13

$$\frac{\partial v(x_i, y_j, t)}{\partial t} = -c_1 * \left(v(x_i, y_j, t) * \left(a - v(x_i, y_j, t)\right) * \left(1 - v(x_i, y_j, t)\right)\right) - c_2 * r(x_i, y_j, t) *$$

$$v(x_i, y_j, t) + I(x_i, y_j, t) + G_x * \frac{\partial^2 v(x_i, y_j, t)}{\partial x^2} + G_y * \frac{\partial^2 v(x_i, y_j, t)}{\partial y^2}$$

$$\frac{\partial r(x_i, y_j, t)}{\partial t} = b * v(x_i, y_j, t) - g * r(x_i, y_j, t) \tag{13}$$

The BC's set as a periodic boundary, which means that the edges of the input array are considered adjacent points. To solve the coupled system equation in time domain represented in Eq.1, we proposed a forward FDM, which was optimised to adaptively sought the most effective time steps for approximating a solution within a relative error tolerance (10^{-5}) and absolute error tolerance (10^{-7}). Wave propagation along a $2 - D, NxM$ neuron array, whose number is $N = M$ in one dimension, can now be simulated. IC's set as $2N^2$ matrix with the first row demonstrating the N^2 initial voltages and the second row the N^2 values of the primary recovery variables. The solver assemble as its output a $tx1$ time vector, and a $tx2N^2$ matrix. By using this configuration, the evolution of the voltage and recovery variables of the neuron array can be tracked as time progresses.

The time derivatives of the SFN equation is approximated via the forward FDM. The second-order partial derivatives concerning x and y directions are subjected to the second-order PDQM. The complete numerical scheme is represented in the light of this information as in Eq.14

$$\frac{v(x_i, y_j, t+\Delta t) - v(x_i, y_j, t)}{\Delta t} = -c_1 * \left(v(x_i, y_j, t) * \left(a - v(x_i, y_j, t)\right) * \left(1 - v(x_i, y_j, t)\right)\right) - c_2 *$$

$$r(x_i, y_j, t) * v(x_i, y_j, t) + I(x_i, y_j, t) + G_x * \sum_{k=1}^{N} \omega_{ik}^{(2)} * v(x_k, y_j, t) + G_y *$$

$$\sum_{k=1}^{M} \overline{\omega}_{jk}^{(2)} * v(x_i, y_k, t)$$

$$\frac{r(x_i, y_j, t+\Delta t) - r(x_i, y_j, t)}{\Delta t} = b * v(x_i, y_j, t) - g * r(x_i, y_j, t) \tag{14}$$

CAGLAR UYULAN

3.2. The relationship between differential quadrature method and the finite difference method

Let us assume that there exists a M grid point in the definition space. Utilising PDQM, one can write the first-order derivative of the function $f(x)$ at the grid point x_i as a linear sum of the function values of the multiplication of the functions at the other grid points with the weight coefficients given in Eq.15.

$$\frac{df(x_i)}{dx} = \sum_{j=1}^{M}\left(w_{ij} * f(x_j)\right), \quad i = 1,2,\ldots,M \tag{15}$$

Since the finite difference scheme depends on the Taylor series expansion, the weight coefficients can be evaluated through Taylor series expansion as in Eq.16.

$$f(x_j) = f(x_i) + (x_j - x_i) * \frac{df(x_i)}{dx} + \cdots + \frac{(x_j-x_i)^k}{k!} * \frac{d^k f(x_i)}{dx^k} + \cdots + \frac{(x_j-x_i)^{(M-1)}}{(M-1)!} * \frac{d^{(M-1)} f(x_i)}{dx^{(M-1)}} +$$

$$E_M \tag{16}$$

where $\quad E_M = \frac{(x_j-x_i)^{(M)}}{(M)!} * \frac{d^{(M)} f(\xi)}{dx^{(M)}}, \xi \in [x_i, x_j]$ is the truncation error.

If we replace Eq.15 into Eq.16, Eq.17 is obtained as

$$\frac{df(x_i)}{dx} = f(x_i) * \sum_{j=1}^{M}(w_{ij}) + \frac{df(x_i)}{dx} * \sum_{j=1}^{M}\left(w_{ij} * (x_j - x_i)\right) + \cdots + \frac{d^k f(x_i)}{dx^k} * \sum_{j=1}^{M}\left(w_{ij} * \right.$$

$$\left. \frac{(x_j-x_i)^k}{k!}\right) + \cdots + \frac{d^{(M-1)} f(x_i)}{dx^{(M-1)}} * \sum_{j=1}^{M}\left(w_{ij} * \frac{(x_j-x_i)^{(M-1)}}{(M-1)!}\right) \tag{17}$$

where

$$\sum_{j=1}^{M}(w_{ij}) = 0, \quad \sum_{j=1}^{M}\left(w_{ij} * (x_j - x_i)\right) = 1, \quad \sum_{j=1}^{M}\left(w_{ij} * \frac{(x_j-x_i)^k}{k!}\right) = 0 \ \ k = 2,3,\ldots,M-1$$

Bellman's first approach, the polynomial $x^k, k = 0,1,\ldots,M-1$ dictates that

$$\sum_{j=1}^{M}(A_{ij}) = 0$$

$$\sum_{j=1}^{M}(A_{ij} * x_j) = 1$$

$$\sum_{j=1}^{M}(A_{ij} * x_j^k) = k * x_i^{k-1}, \quad i = 1,2,\ldots,M, \quad k = 2,3,\ldots,M-1$$

In this way, weight coefficients of the high order finite difference scheme can be calculated for the

first-order derivative. The higher order derivatives are also evaluated with the PDQM mentioned above as in Eq.18

$$\frac{d^m f(x_i)}{dx^m} = f(x_i) * \sum_{j=1}^{M}\left(A_{ij}{}^m\right) + \cdots + \frac{d^k f(x_i)}{dx^k} * \sum_{j=1}^{M}\left(A_{ij}{}^m * \frac{(x_j - x_i)^k}{k!}\right) + \cdots + \frac{d^{(m)} f(x_i)}{dx^{(m)}} *$$

$$\sum_{j=1}^{M}\left(A_{ij}{}^m * \frac{(x_j - x_i)^{(m)}}{(m)!}\right) \qquad i = 1,2,\ldots,M \; ; m = 2,3,\ldots,M-1 \tag{18}$$

where

$$\sum_{j=1}^{M}\left(A_{ij}\right)^m = 0, \qquad \sum_{j=1}^{M}\left(A_{ij}{}^m * \left(x_j - x_i\right)^m\right) = m!, \qquad \sum_{j=1}^{M}\left(A_{ij}{}^m * \frac{(x_j - x_i)^k}{k!}\right) = 0$$

$$k = 1,2,\ldots,M-1, \quad k \neq m$$

Accordingly, it can be deduced that PDQM can obtain the weight coefficients in the high-order finite difference scheme. In other words, it can be seen that PDQM is equivalent to the high-order finite difference scheme. The weight coefficients obtained from one of the sets of base vectors are equal to the weight coefficients obtained from another set of base vectors. Therefore, equation systems that determine the weight coefficients will be identical. The proof that the equations derived from PDQM and finite difference scheme are equal is given in APPENDIX-II. These methods can be applied to both internal points and boundary points. Also, regular or irregular grid points do not prevent the application of the technique.

3.3. Implementation Methodology of Boundary Conditions

The implementation of BC's is crucial to obtain accurate solutions. The PDQ algebraic equations are stated in a matrix form as in Eq.19

$$[A]\{\overline{v}\} = \{b\} \tag{19}$$

where $\{\overline{v}\} = \{v; r\}$ is a vector of unknown $2(N * M)$ functional values at all discretised points of the domain, $[A]$ is $2(N * M) \times 2(N * M)$ coefficient matrix including the weighting coefficients $\omega_{ik}^{(2)}$, $\overline{\omega}_{jk}^{(2)}$, and $\{b\}$ is the $2(N * M) \times 1$-sized right-hand side vector comprising first-order time derivatives of the function $\overline{v}$.

The Dirichlet type BC's are inserted directly because the known values contribute to the right-hand side vector $\{b\}$. When the BC's, which covers the normal derivatives of the unknown function $\overline{v}$ exists, the derivatives are also approximated through PDQM.

Dirichlet Type BC's:

Dirichlet type BC should be applied at the interior points since the solution at the boundary grid points is known. The Eq.13 can be reshaped as in Eq.20.

$$\frac{v(x_i,y_j,t+\Delta t)-v(x_i,y_j,t)}{\Delta t} = -c_1 * \left(v(x_i,y_j,t) * \left(a - v(x_i,y_j,t)\right) * \left(1 - v(x_i,y_j,t)\right)\right) - c_2 *$$

$$r(x_i,y_j,t) * v(x_i,y_j,t) + I(x_i,y_j,t) + G_x * \sum_{k=2}^{N-1} \omega_{ik}^{(2)} * v(x_k,y_j,t) + G_y *$$

$$\sum_{k=2}^{N-1} \overline{\omega}_{jk}^{(2)} * v(x_i,y_k,t) + D_{ij} \tag{20}$$

where $2 \leq i \leq N - 1, \ 2 \leq j \leq M - 1$

$$D_{ij} = \omega_{i1}^{(2)}v(x_1,y_j,t) + \omega_{iN}^{(2)}v(x_N,y_j,t) + \overline{\omega}_{j1}^{(2)}v(x_i,y_1,t) + \overline{\omega}_{jM}^{(2)}v(x_i,y_M,t)$$

Eq.20 can be evaluated by using iterative methods for discrete-time derivative values of v after the time derivative is discretised.

Neumann Type BC's:

The normal derivative of the $v(x,y,t)$ can be obtained as

$$\frac{\partial v(x,y,t)}{\partial n} = \frac{\partial v(x,y,t)}{\partial x} * \overrightarrow{n_x} + \frac{\partial v(x,y,t)}{\partial y} * \overrightarrow{n_y}$$

For the Neumann conditions, the normal derivatives on the boundary are also discretised by PDQM as in Eq.21

$$\frac{\partial v(x_i,y_j,t)}{\partial x} = \sum_{k=1}^{N} \omega_{ik}^{(1)} * v(x_k,y_j,t) \qquad\qquad i = 1,2,\dots,N$$

$$\frac{\partial v(x_i,y_j,t)}{\partial y} = \sum_{k=1}^{M} \overline{\omega}_{jk}^{(1)} * v(x_i,y_k,t) \qquad\qquad j = 1,2,\dots,M \tag{21}$$

Assuming $\frac{\partial v(x_N,y_j,t)}{\partial x} = c_j \quad (j = 1,2,\dots,M)$ and $\frac{\partial v(x_N,y_j,t)}{\partial y} = 0$ are given on one part of the boundary; it can be written as in Eq.22

$$\frac{\partial v(x_N,y_j,t)}{\partial x} = \sum_{k=1}^{N} \omega_{Nk}^{(1)} * v(x_k,y_j,t) = \omega_{NN}^{(1)} * v(x_N,y_j,t) + \sum_{k=1}^{N-1} \omega_{Nk}^{(1)} * v(x_k,y_j,t) = c_j \tag{22}$$

$v(x_N,y_j,t)$ is obtained as a value on the boundary as in Eq.23

$$v(x_N,y_j,t) = \frac{1}{\omega_{NN}^{(1)}}\left(c_j - \sum_{k=1}^{N-1} \omega_{Nk}^{(1)} * v(x_k,y_j,t)\right) \qquad j = 1,2,\dots,M \tag{23}$$

These M equations for the unknowns $v(x_N,y_j,t), j = 1,2,\dots,M$ are replaced to the Eq.19 which is written for $i \neq N, \ j = 1,2,\dots,M$ for the case of Neumann type of BC's $\frac{\partial v(x_N,y_j,t)}{\partial x} = c_j$ on

$x = x_N, (i = N)$.

The mixed type BC's combined with the Dirichlet and Neumann BC's are applied similarly.

4. MAIN RESULTS

Simulations are conducted via Matlab code, which describes a monodomain reaction-diffusion model in 2-D. SFN equations are constructed to simulate the spiral wave-shaped neuron AP. The progression of the two normalised state variables, membrane voltage $v(x, y, t)$ moreover, recovery $r(x, y, t)$, is computed across a <u>128×128</u> spatial domain and across time. Two different pacing methods were selected to initiate the spiral waves

1) *two-point stimulation* where a point stimulus is delivered in the centre of the domain followed by another point stimulus on the partially refractory wake of the first wave of excitation.

2) *cross-field stimulation* where a stimulus is applied to the left domain boundary causing a plane wave. As this wave travels across the domain, a second stimulus is applied to the bottom boundary of the domain.

As the simulations run the activation state of the individual units comprising the domain is mapped to colour and plotted in a figure window. A count of time steps is displayed at the top of the plot. Model equations are solved using PDQM for spatial derivatives and FDM for time derivatives. A movie file in .AVI format is produced after simulation conducted in Matlab. One simulation takes about 120 seconds on an Intel Core i7-6700HQ CPU 2.60 GHz. 64-bit Laptop.

Model parameters are represented in Table 1.

Table 1: Membrane parameters of the SFN neuron model.

$$a = 0.13$$
$$b = 0.013$$
$$c_1 = 0.26$$
$$c_2 = 0.1$$
$$\gamma = 0.013$$
$$G_x = G_y = 1 \ (isotropic \ assumption)$$

The diffusive terms "$G_x \ and \ G_y$" control the passive spread of current. The ionic currents are

defined by b, γ, c_1 and c_2 terms, respectively. The activation function is governed by the cubic term $f(v(x, y, t))$. There exist three fixed points at $v = 0, v = a$ and $v = 1$. The points $v = 0$ and $v = 1$ are stable and responsible for the resting and excited states. The excitation threshold, which makes the Eq.1 unstable at point $v = a$, is represented by a. A point in the domain evolves to $v = 0$ unless the fluctuations dominate the excitation threshold. The refractory variable r pulls the system to the resting state and prohibits the re-excitation for a certain recovery period. When the parameters are selected suitably, local state vibrates around resting, excitation and refractory zones [51].

4.1. Action potential propagation without diffusion

First of all, the AP without diffusion is investigated by using the parameters given in Table 1. The stimulus pattern to initiate the AP is given in Fig.1
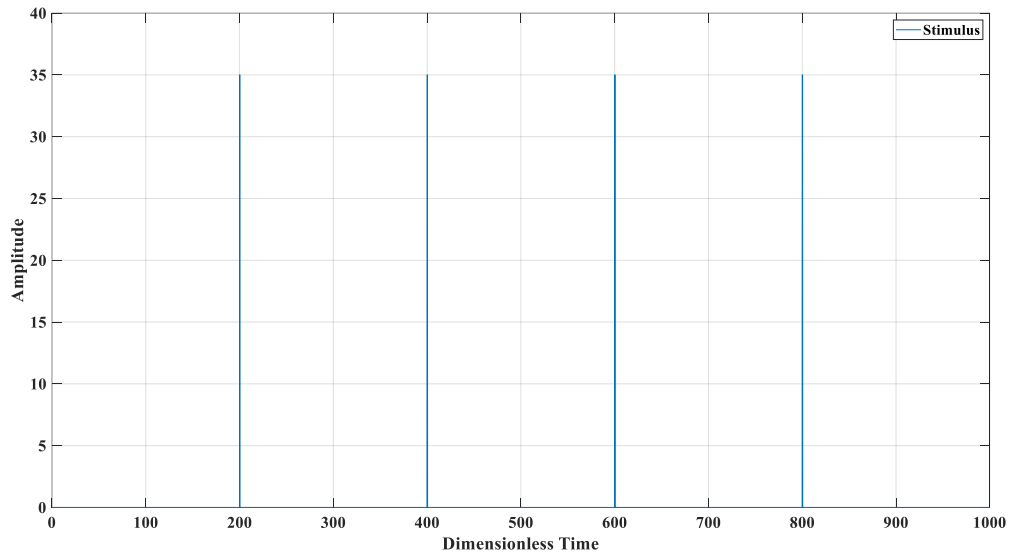

Figure 1: The stimulus pattern for starting AP (The width of the impulse stimulus is 0.5).

These instants are chosen so that the full profile of AP can be captured. The AP waveforms and phase portrait of the excitation and recovery variables were given in Fig.2a and Fig.2b., respectively.
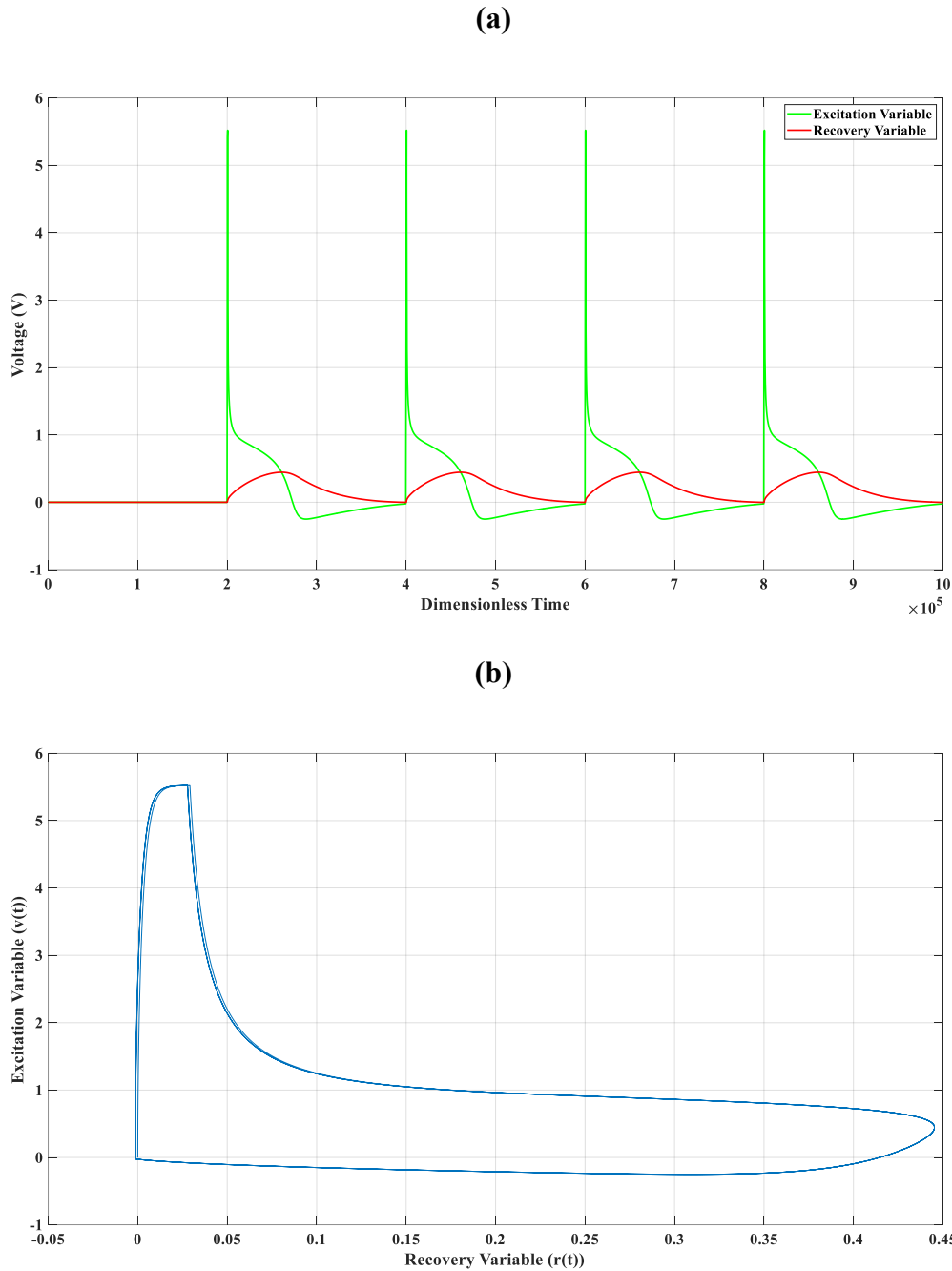
(a)

(b)

Figure 2: a) Traveling SFN waves in one dimension or AP profiles in time domain $v(t), r(t)$, b) corresponding phase portraits.

The waveform of $v(t)$ exhibits a negative trend during the refractory state of the wave. While $v(t)$ approaches to zero, $r(t)$ is elevated.

4.2. Action potential propagation with diffusion

$2-D$ domain is chosen as a square shape, whose number of columns $(x-direction)$ and some

rows in $(y - \text{direction})$ are 128 with a grid (mesh) size 1. The total number of time steps in a full simulation (duration) is 25000, with a 0.15-time step in each iteration. The code of the stimulation protocols is given in APPENDIX-III for two-point and cross-field stimulation.

Case 1: Spiral waves initiated by two-point stimulation

In this case, two different types of stimulus $I_1 = 2 * \text{threshold}$ and $I_2 = 5 * \text{threshold}$ is applied to a different location and different time. First I_1 wave is initiated at the position given in Fig.3a; then it propagates through the domain (Fig. 3b, Fig.3c). Then, I_2 is induced, resulting in elliptical wavefront due to the anisotropy of the array (Fig.3d, Fig.3e). As a result, a pair of self-sustaining counter-rotating spirals are created (Fig.3f, Fig.3g). As time advances, the two tails of the spiral collide and, this process gives rise to another cyclic spiral wave (Fig.3h, Fig.3i, Fig.3j). The frames regarding this periodic shape are given in Fig3k, Fig3l, Fig.3m, respectively

(a)   (b)   (c)

(d)   (e)   (f)
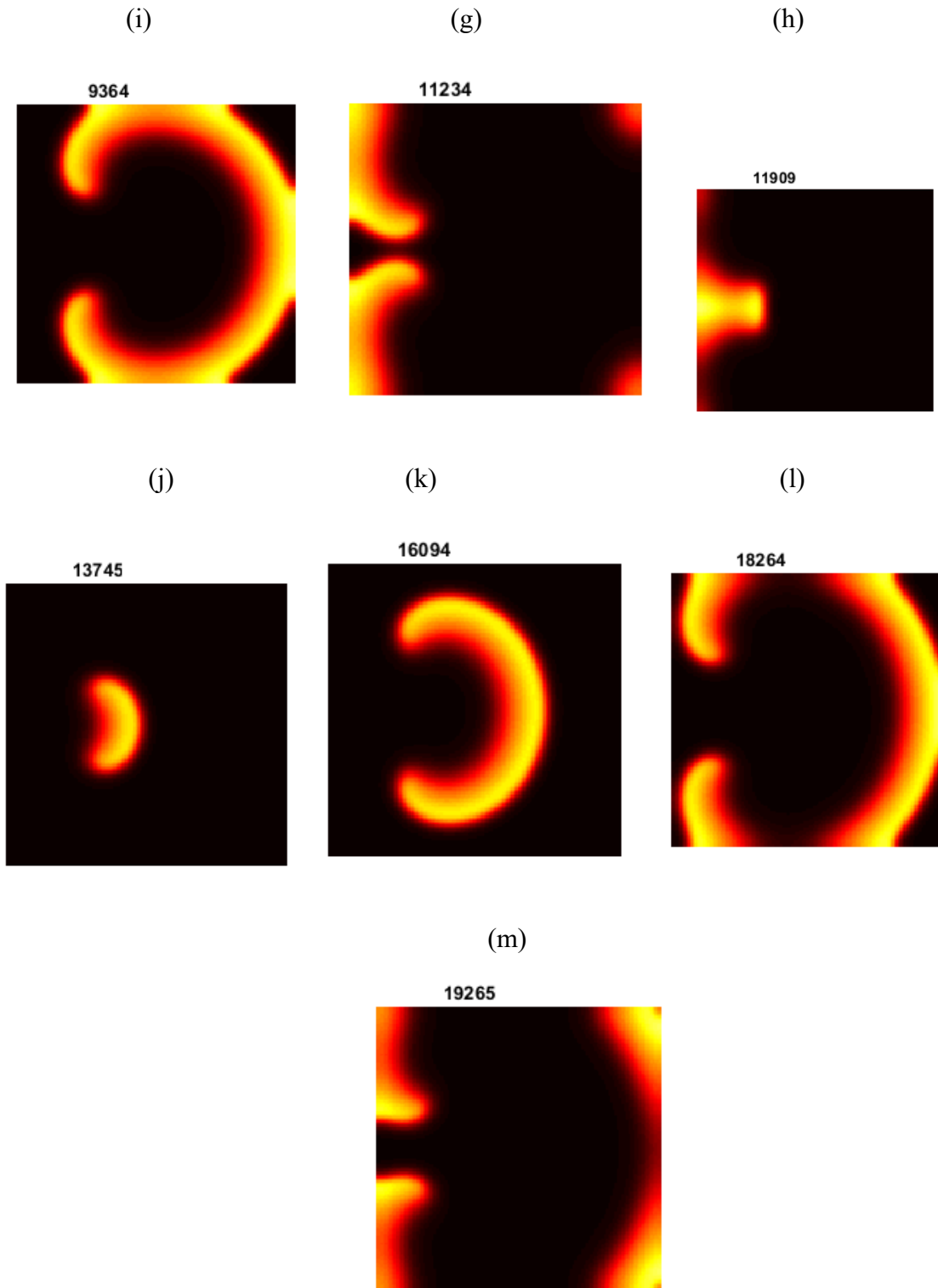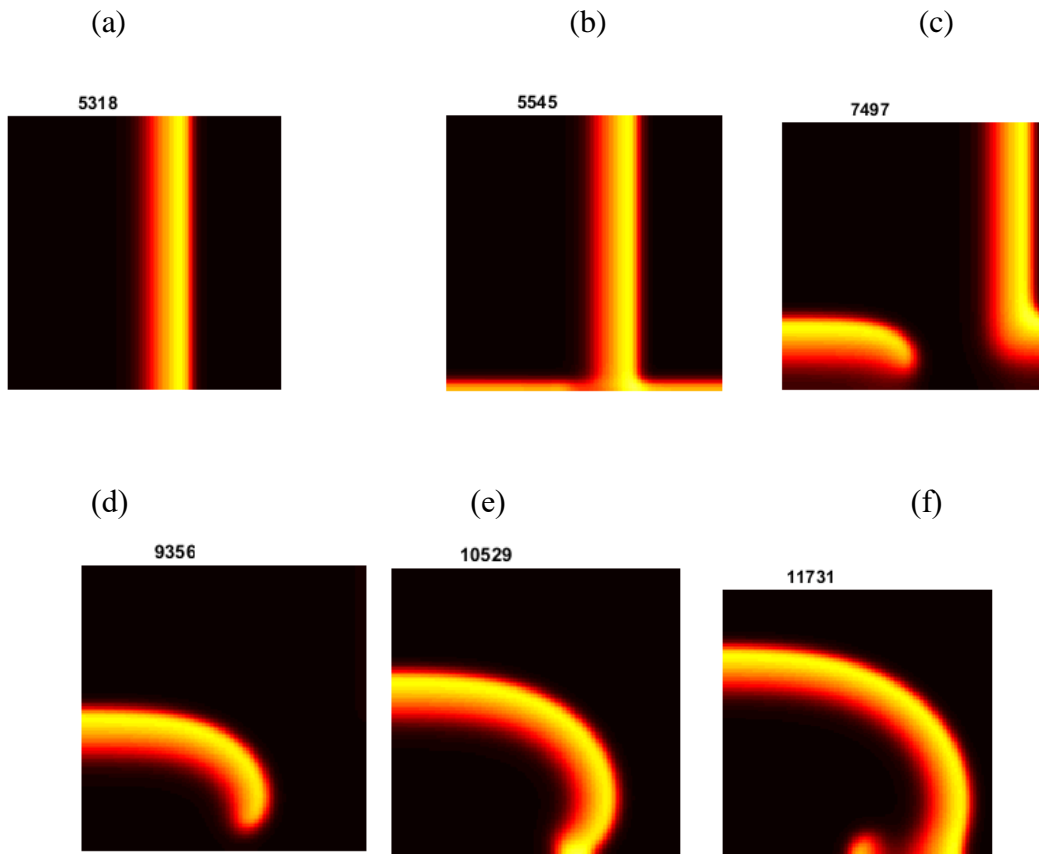
(i)   (g)   (h)

(j)   (k)   (l)

(m)
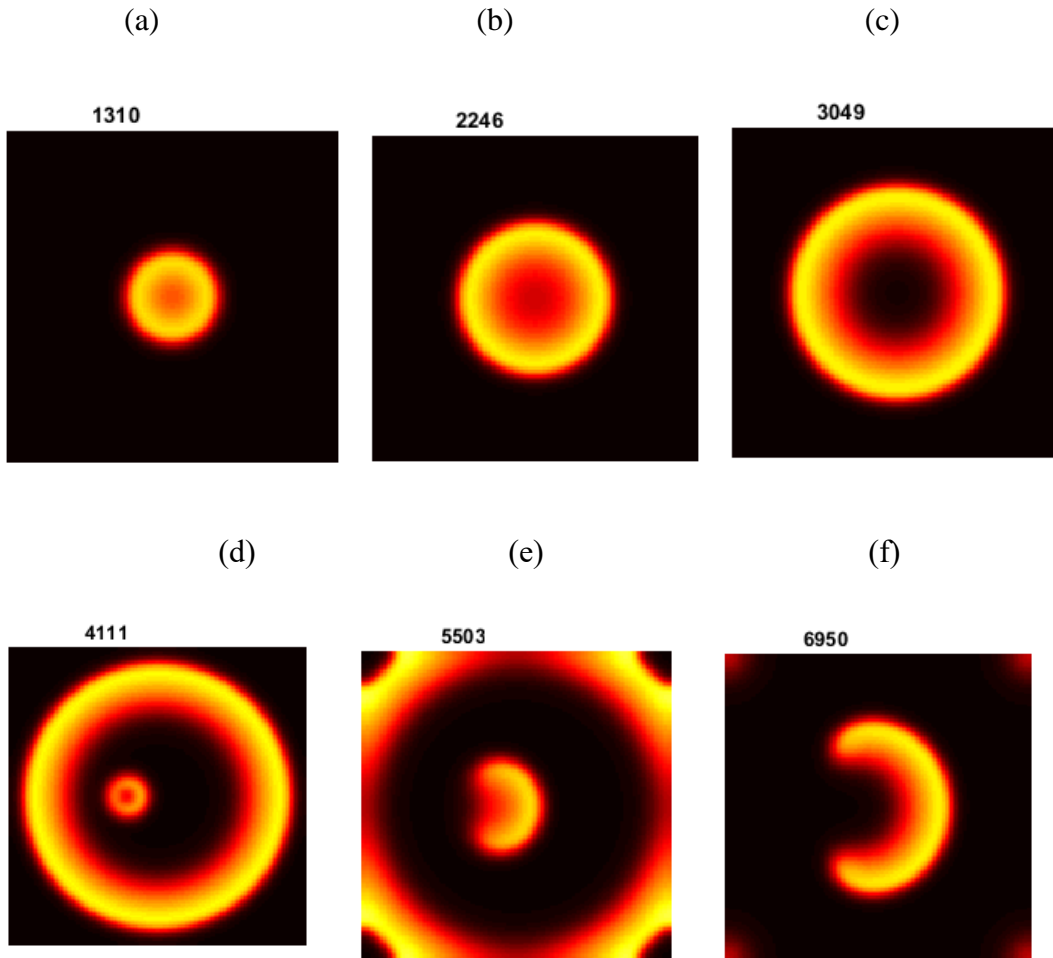
Figure 3: Video frames are presenting the initiation of spiral wave activity in two-dimensional neuron array of FitzHugh-Nagumo excitable cells subjected to two-point stimulation.

Case 2: Spiral waves initiated by cross-field stimulation

In this case, a conditioning stimulus ($I_1 = 2 *$ threshold) applied to the whole column of cells on the left border of the array, initiated a planar wave which advances with a uniform velocity toward the right (Fig.4a). Then, a test stimulus ($I_2 = 5 *$ threshold) is activated perpendicularly to I_1 moreover, a second planar wave, which propagates upward, where it coincided with the refractory end of I_1 (Fig.4b, Fig.4c). I_2 wave enters to the curl phase toward the right (Fig.4d, Fig.4e). In Fig.4f and Fig.4g, the subsequent changes of the I_2 wave is represented as it rotates clockwise. A self-sustaining activity, which generates a transient discontinuity in the propagating wave, can be induced in a 2-D excitable domain (Fig.4h, Fig.4i, Fig.4j). The timing of the stimulus I_2 cause the position of both the break pattern and the centre of rotation of the spiral wave.

(a)   (b)   (c)

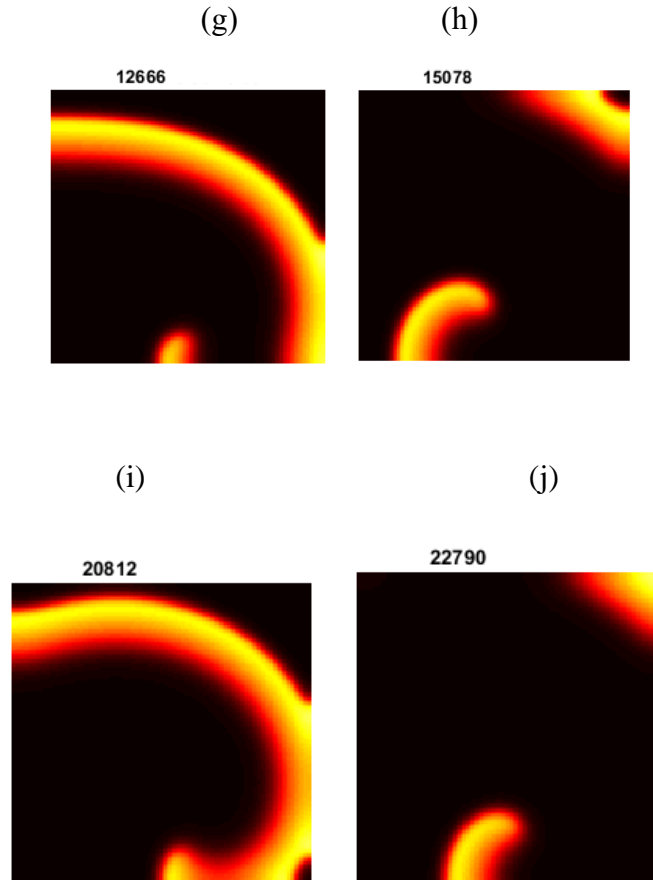(d)   (e)   (f)

(g)   (h)

(i)   (j)

Figure 4: Video frames are presenting the initiation of spiral wave activity in two-dimensional neuron array of FitzHugh-Nagumo excitable cells subjected to cross-field stimulation.

The branching nature of AP is explored in the simulation. Thus, it can be predicted when the two APs travelling in opposite directions coincided. It can also be deduced that the refractory zones block two colliding pulses from passing through each other. The FHN model simulation shows that the pulses eliminate each other upon collision. Spiral waves, which are self-sustained waves of excitation, rotate around an obstacle and repeats its activating sequence with a determined frequency. Spiral waves might break up into smaller waves [52-54].

Case 3: Spiral waves initiated by mixed BC's for two-point stimulation case

In this case, the stimulation process is the same as Case 1, but the BC's are set mixed as given below.

Dirichlet BC's

$$v(0,y,t) = 0, \quad v(N,y,t) = \frac{1}{2} + \frac{1}{2}\tanh\left(\frac{1}{2\sqrt{2}}\left(N - \frac{2a-1}{\sqrt{2}}t\right)\right)$$

$$v(x,0,t) = 0, \quad v(x,M,t) = \frac{1}{2} + \frac{1}{2}\tanh\left(\frac{1}{2\sqrt{2}}\left(M - \frac{2a-1}{\sqrt{2}}t\right)\right) \quad , \quad t \in [0,T]$$

Neumann BC's

$$\frac{\partial v(0,y,t)}{\partial x} = 0, \quad \frac{\partial v(N,y,t)}{\partial x} = \frac{1}{2} + \frac{1}{2}\tanh\left(\frac{1}{2\sqrt{2}}\left(N - \frac{2a-1}{\sqrt{2}}t\right)\right) \qquad\qquad ,t \geq 0$$

$$\frac{\partial v(x,0,t)}{\partial y} = 0, \quad \frac{\partial v(x,M,t)}{\partial y} = \frac{1}{2} + \frac{1}{2}\tanh\left(\frac{1}{2\sqrt{2}}\left(M - \frac{2a-1}{\sqrt{2}}t\right)\right) \qquad\qquad ,t \geq 0$$
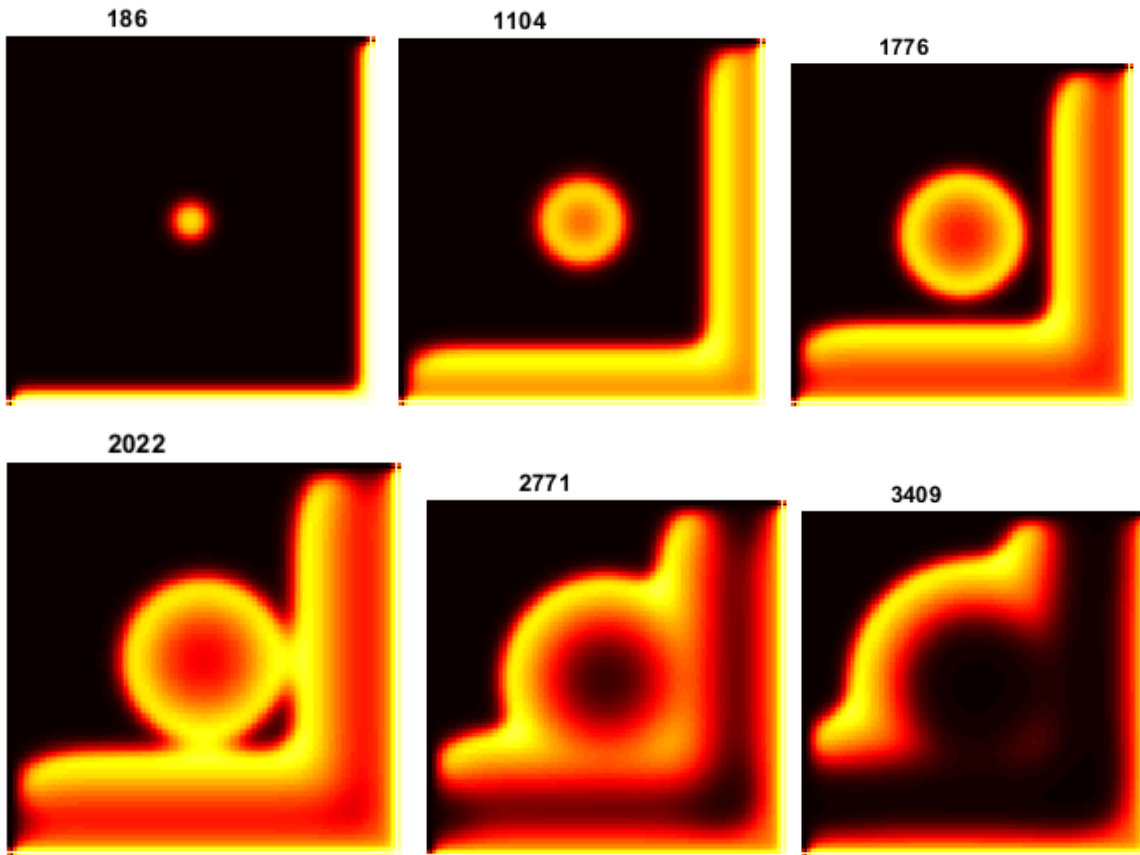
Subject to the IC

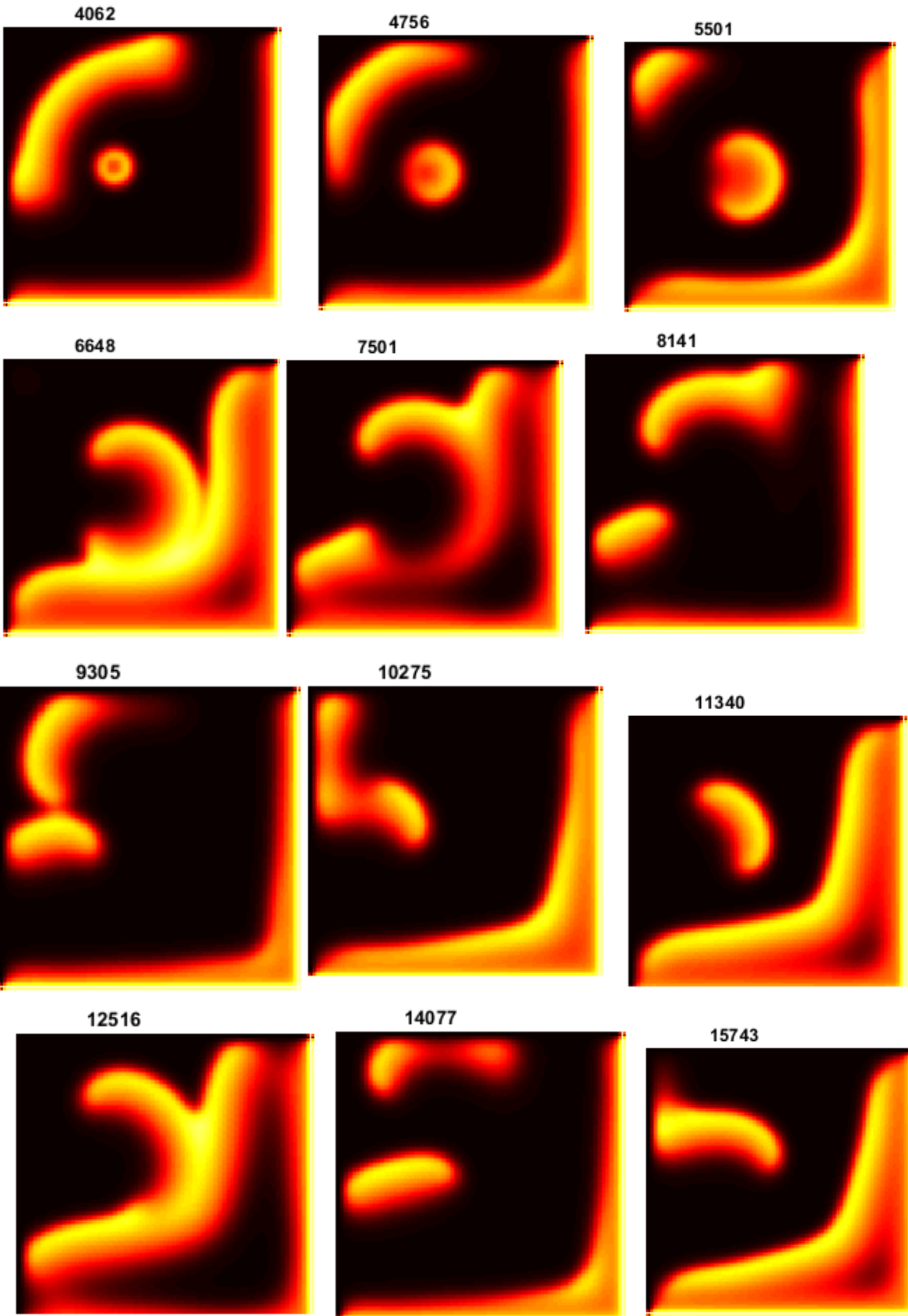$$v(x,y,0) = \hat{h}(x,y) \qquad\qquad , \quad 0 \leq x \leq N, 0 \leq y \leq M$$

where $\hat{h}(x,y) = [\frac{1}{2} + \frac{1}{2}\tanh\left(\frac{x}{2\sqrt{2}}\right), \frac{1}{2} + \frac{1}{2}\tanh\left(\frac{y}{2\sqrt{2}}\right)]$

where (x,y) represents the spatial coordinates, t indicates the time.

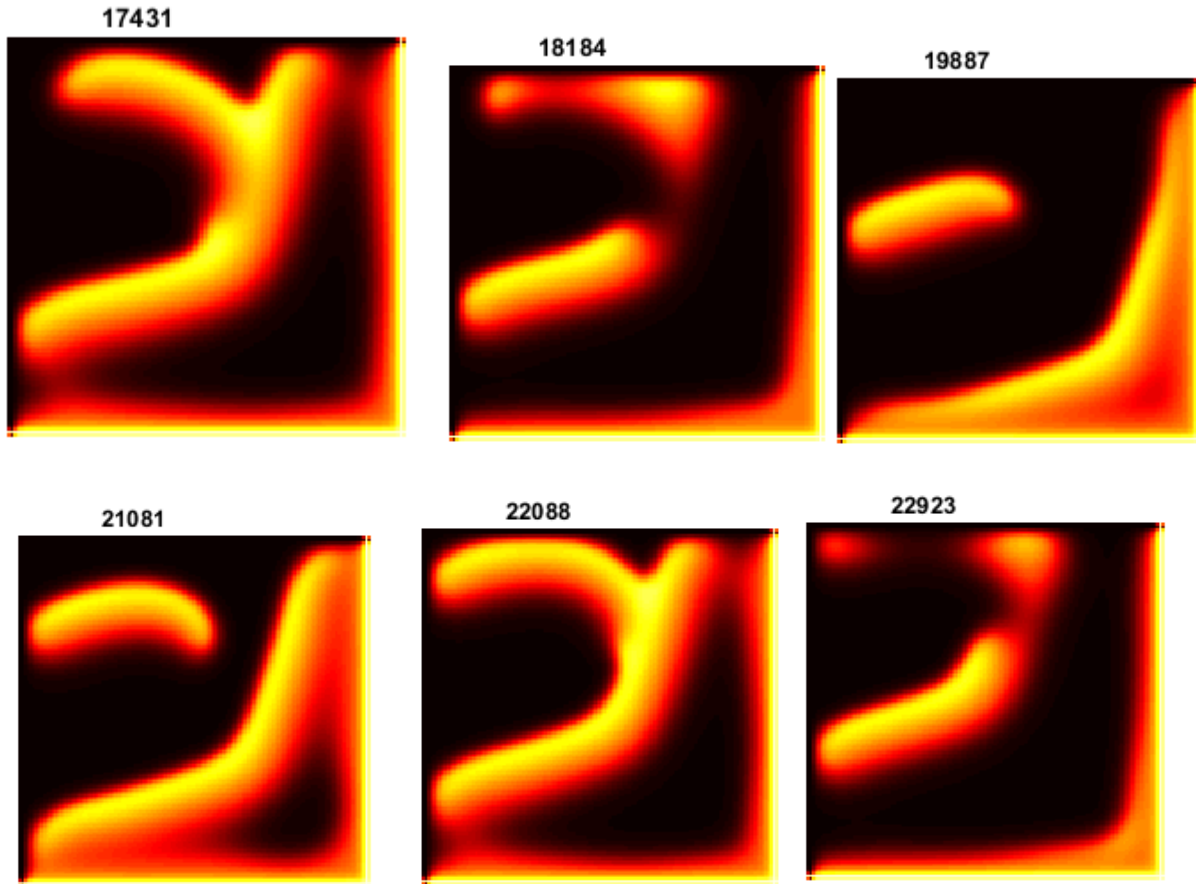The evolution of wave propagation is represented in Fig.5.

Figure 5: Video frames are presenting the initiation of spiral wave activity in two-dimensional neuron array of FitzHugh-Nagumo excitable cells subjected to two-point stimulation with mixed BC's.

5. CONCLUSION

In this paper, the numerical solutions of the excitable neuron array are derived from the SFN equations, which reveals the dynamical behaviour of the neuron excitability and spiral wave activity. The fast and slow variables of the HH model is reduced for simplicity as an SFN model. Travelling wave pulse solutions are presented using PDQM for two-point and cross-field stimulation in the system having Neumann-type BCs, and Dirichlet-Neumann-type mixed BC's, respectively. It is possible to reproduce/mimic the dynamic systems of the electrophysiological description of neuronal activity by numerical simulation. The simulation methodology demonstrates a predictive model of AP propagation, whose properties comprise branching and

collision. The effects of diffusion on the travelling speed and wavefront width can also be captured via presented simulation. It is also possible to research the dynamics coupled with an electrode stimulus.

The main contribution of this paper is that a novel hybrid PDQM and FDM-based numerical approach was adapted to solve the nonlinear SFN equation. This method can be implemented to find solutions for other nonlinear PDE's which emerges in engineering, mathematical physics. The simulation results are found to be in good agreement with the literature.

In the future works, a detailed parametric analysis will be investigated to capture the chaotic neuron dynamics emerged from SFN equation and next step is to simulate a rich set of neural firing behaviour through a 3-D model by using the tools of quantitative and geometric/graphical dynamical system analysis (stability, chaos and bifurcation etc.).

CONFLICT OF INTERESTS

The authors declare that there is no conflict of interests.

APPENDIX-I

```
function [A,B,C,D,X]=DQSS(N,p,q)
% [p q] Domain
for i=1:N
X(i)=(0.5*(1-cos((i-1)*pi/(N-1)))); % CGL Grid Points
end
%for i=1:N
%X(i)=(i-1)/(N-1);
%end
X=normalize_var(X,p,q); ***
Y=ones(N);
for i=1:length(X)    % length(xx)=N
```

```
Y(i)=1;

for k=1:N

if(k~=i)

Y(i)=Y(i)*(X(i)-X(k));

end

end

end

% Weighted Coefficient [Aij] Shu's Approach NxN matrix (1)

A=zeros(N);

for i=1:N

for j=1:N

if(j~=i)

A(i,j)=Y(i)/((X(i)-X(j))*Y(j));

A(i,i)=A(i,i)-A(i,j); % First Order Weighted Coefficients

end

end

end

% Weighted Coefficient [Bij] Shu's Approach NxN matrix (2)

B=zeros(N);

l=2;

for i=1:N

for j=1:N

if(j~=i)

B(i,j)=l*(A(i,j)*A(i,i)-A(i,j)/(X(i)-X(j)));

B(i,i)=B(i,i)-B(i,j); % Second Order Weighted Coefficients

end

end
```

```
end

% B=A*A;

% Weighted Coefficient [Cij] (3) Shu's Approach NxN matrix    (3)

C=zeros(N);

m=3;

for i=1:N

for j=1:N

if(j~=i)

C(i,j)= m*(A(i,j)*B(i,i)-B(i,j)/(X(i)-X(j)));

C(i,i)=C(i,i)-C(i,j); % Third order Weighted Coefficients

end

end

end

% C=A*B;

% Weighted Coefficient [Dij](4) Shu's Approach NxN matrix (4)

D=zeros(N);

n=4;

for i=1:N

for j=1:N

if(j~=i)

D(i,j)= n*(A(i,j)*C(i,i)-C(i,j)/(X(i)-X(j)));

D(i,i)=D(i,i)-D(i,j); % Fourth Order Weighted Coefficients

end

end

end

%D=A*C;

end
```

***function normalized = normalize_var(array, x, y)

% Normalize to [0, 1]:

m = min(array);

range = max(array) - m;

array = (array - m) / range;

% Then scale to [x,y]:

range2 = y - x;

normalized = (array*range2) + x;

end

APPENDIX-II

$i, j = 1, 2, \ldots, M$ and $m = 2, 3, \ldots, M - 1$

$$\left(A_{ij}\right)^m = m\left(w_{ij} * A_{ii}{}^{m-1} - \frac{\left(A_{ij}\right)^{m-1}}{x_i - x_j}\right)$$

For $m = 1$

$$\sum_{j=1}^{M}\left(A_{ij}\right)^m = \sum_{j=1}^{M}\left(w_{ij}\right)^m = 0$$

For $2 \le m \le M - 1$

$$\sum_{j=1}^{M}\left(\left(A_{ij}\right)^{m-1} * \left(x_j - x_i\right)^k\right) = \begin{cases} (m-1)!, & k = m - 1 \\ 0, & k \ne m - 1 \end{cases}$$

For $1 \le k \le M - 1$

$$\sum_{j=1}^{M}\left(\left(A_{ij}\right)^m * \left(x_j - x_i\right)^k\right) = \sum_{j=1}^{M}\left(\left[m * w_{ij} * (A_{ii})^{m-1} - m * \frac{\left(A_{ij}\right)^{m-1}}{x_i - x_j}\right] * \left(x_j - x_i\right)^k\right) = m *$$

$$(A_{ii})^{m-1} * \sum_{j=1}^{M}\left(w_{ij} * \left(x_j - x_i\right)^k\right) + m * \sum_{j=1}^{M}\left(\left(A_{ij}\right)^{m-1} * \left(x_j - x_i\right)^{k-1}\right) =$$

$$m * \sum_{j=1}^{M}\left(\left(A_{ij}\right)^{m-1} * \left(x_j - x_i\right)^{k-1}\right)$$

$$\sum_{j=1}^{M}\left(\left(A_{ij}\right)^m * \left(x_j - x_i\right)^k\right) = \begin{cases} m!, & k = m \\ 0, & otherwise \end{cases}$$

APPENDIX-III

deltat=1e-3;

tend=25000*deltat;

```
t=0:deltat:tend;

N=128; % Number of grid points in x-dimension

M=128; % Number of grid points in y-dimension

% Set initial stimulation current and pattern

threshold=10;

I_stim_1=2*threshold;

I_stim_2=5*threshold;

i_stim=zeros(N,M);

if StimulationProtocol==1

i_stim(N/2:N/2+5,M/2:M/2+5)=I_stim_1;

else

i_stim(:,1)=I_stim_1;

end

n1e=20*deltat; % Step at which to end 1st stimulus

switch StimulationProtocol

case 1 % Two-point stimulation

n2b=3800*deltat; % Step at which to begin 2nd stimulus

n2e=3900*deltat; % Step at which to end 2nd stimulus

case 2 % Cross-field stimulation

n2b=5400*deltat; % Step at which to begin 2nd stimulus

n2e=5420*deltat; % Step at which to end 2nd stimulus

end

while ~done % Time loop

if n == n1e % End 1st stimulus

i_stim=zeros(N,M);

end

if n == n2b % Begin 2nd stimulus
```

```
switch StimulationProtocol

case 1

i_stim(N/2:N/2+5,M/2:M/2+5)=I_stim_2;

case 2

i_stim(end,:)=I_stim_2;

end

end

if n == n2e % End 2nd stimulus

i_stim=zeros(N,M);

end
```

REFERENCES

[1] S. Nadeem, N. S. Akbar, Effects of heat transfer on the peristaltic transport of MHD Newtonian fluid with variable viscosity: Application of Adomian decomposition method. Commun. Nonlinear Sci. Numer. Simul. 14(11)(2009), 3844-3855.

[2] R. Fitzhugh, Impulses and the Physiological States in Theoretical Models of Nerve Membrane. Biophys. J. 1(6)(1961), 445-466.

[3] H. Wilhelmsson, Simultaneous diffusion and reaction processes in plasma dynamics. Phys. Rev. A, 38(3)(1988), 1482-1489.

[4] G. W. Griffiths, W. E. Schiesser, Traveling wave analysis of partial differential equations: Numerical and analytical methods with MATLAB and Maple. Academic Press, Amsterdam, 2012.

[5] G. Rigatos, Advanced Models of Neural Networks Nonlinear Dynamics and Stochasticity in Biological Neurons. Springer, Berlin, 2016.

[6] C. Jones, R. Gardner, J. Alexander, A topological invariant arising in the stability analysis of travelling waves. J. Reine Angew. Math. 410 (1990), 168-212.

[7] E.M. Izhikevich, Dynamical Systems in Neuroscience: The Geometry of Excitability and Bursting. MIT Press, Cambridge, 2014.

[8]   J. Cronin, Mathematical aspects of Hodgkin-Huxley neural theory, Cambridge University Press, Cambridge [Cambridgeshire]; New York, 1987.

[9]   J.P. Keener, J. Sneyd, Mathematical physiology, Springer, New York, NY, 2008.

[10] A. Castellanos, B. Portillo, J. Mejias, N. Leon-Portillo, N.C. Saoudi, L. Zaman, Entrainment of circus movement tachycardia utilizing an accessory pathway with long retrograde conduction times during ventricular and atrial stimulation, J. Amer. Coll. Cardiol. 6 (1985), 1431–1437.

[11] H.C. Tuckwell, L.M. Ricciardi, A. Buonocore, E. Pirozzi, Mathematical Modeling of Spreading Cortical Depression: Spiral and Reverberating Waves, in: AIP Conference Proceedings, AIP, Vietri sul Mare (Italy), 2008: pp. 46–64.

[12] J.B. Ackman, T.J. Burbridge, M.C. Crair, Retinal waves coordinate patterned activity throughout the developing visual system, Nature. 490 (2012), 219–225.

[13] E.P. Zemskov, A.Yu. Loskutov, Traveling waves in a piecewise-linear reaction-diffusion model of excitable medium, BIOPHYSICS. 54 (2009), 631–636.

[14] J. Gomatam, P. Grindrod, Three-Dimensional Waves in Excitable Reaction-Diffusion Systems: the Eikonal Approximation. In: Holden A.V., Markus M., Othmer H.G. (eds) Nonlinear Wave Processes in Excitable Media. NATO ASI Series (Series B: Physics), vol 244. Springer, Boston, MA, (1991).

[15] T. Bánsági, V.K. Vanag, I.R. Epstein, Two- and three-dimensional standing waves in a reaction-diffusion system, Phys. Rev. E. 86 (2012), 045202.

[16] T. Plesser, R.D. Kingdon, K.H. Winters, The Simulation of Chemical Waves in Excitable Reaction-Diffusion-Convection Systems by Finite Difference and Finite Element Methods. In: Holden A.V., Markus M., Othmer H.G. (eds) Nonlinear Wave Processes in Excitable Media. NATO ASI Series (Series B: Physics), vol 244. Springer, Boston, MA, (1991).

[17] E.M. Ortigosa, L.F. Romero, J.I. Ramos, Spiral waves in three-dimensional excitable media with light-sensitive reaction, Chaos Solitons Fractals. 18 (2003), 365–373.

[18] M. Markus, M. Krafczyk, B. Hess, Randomized Automata for Isotropic Modelling of two- and Three-Dimensional Waves And Spatiotemporal Chaos in Excitable Media. In: Holden A.V., Markus M., Othmer H.G.

(eds) Nonlinear Wave Processes in Excitable Media. NATO ASI Series (Series B: Physics), vol 244. Springer, Boston, MA, (1991).

[19] J. Gomatam, P. Grindrod, Three-dimensional waves in excitable reaction-diffusion systems. J. Math. Biol. 25 (6) (1987), 611-622.

[20] N. Bessonov, A. Beuter, S. Trofimchuk, V. Volpert, Estimate of the travelling wave speed for an integro-differential equation, Appl. Math. Lett. 88 (2019), 103–110.

[21] A. Karma, Scaling regime of spiral wave propagation in single-diffusive media, Phys. Rev. Lett. 68 (1992), 397–400.

[22] J. Nagumo, S. Arimoto, S. Yoshizawa, An Active Pulse Transmission Line Simulating Nerve Axon, Proc. IRE. 50 (1962), 2061–2070.

[23] K.H.W.J. ten Tusscher, A.V. Panfilov, Influence of nonexcitable cells on spiral breakup in two-dimensional and three-dimensional excitable media, Phys. Rev. E. 68 (2003), 062902.

[24] F. Xie, Z. Qu, J.N. Weiss, A. Garfinkel, Interactions between stable spiral waves with different frequencies in cardiac tissue, Phys. Rev. E. 59 (1999), 2203–2205.

[25] J. Rinzel, J. B. Keller, Travelling wave solutions of a nerve conduction equation. Biophys. J. 13(12) (1973), 1313-1337.

[26] J. Manafian, M. Lakestani, New Improvement of the Expansion Methods for Solving the Generalized Fitzhugh-Nagumo Equation with Time-Dependent Coefficients. Int. J. Eng. Math. 2015 (2015), 107978.

[27] F. Liu, P. Zhuang, I. Turner, V. Anh, K. Burrage, A semi-alternating direction method for a 2-D fractional FitzHugh–Nagumo monodomain model on an approximate irregular domain, J. Comput. Phys. 293 (2015), 252–263.

[28] L. Zhang, Existence, uniqueness and exponential stability of travelling wave solutions of some integral differential equations arising from neuronal networks. J. Differ. Equ. 197 (2004), 162-196.

[29] T. Erneux, G. Nicolis, Propagating waves in discrete bistable reaction-diffusion systems, Physica D: Nonlinear Phenomena. 67 (1993), 237–244.

[30] C. Shu, Differential quadrature and its application in engineering, Springer, New York, 2000.

[31] X. Wang, Differential quadrature and differential quadrature based element methods: theory and applications, 2015.

[32] B.K. Singh, A novel approach for numeric study of 2D biological population model, Cogent Math. 3 (2016), 1261527.

[33] X. Wang, C.W. Bert, A New Approach In Applying Differential Quadrature To Static And Free Vibrational Analyses Of Beams And Plates, J. Sound Vibration. 162 (1993), 566–572.

[34] Ö. Civalek, Application of differential quadrature (DQ) and harmonic differential quadrature (HDQ) for buckling analysis of thin isotropic plates and elastic columns, Eng. Struct. 26 (2004), 171–186.

[35] H. Du, M.K. Lim, R.M. Lin, Application of generalized differential quadrature to vibration analysis, J. Sound Vibration. 181 (1995), 279–293.

[36] X. Wang, C.W. Bert, A.G. Striz, Differential quadrature analysis of deflection, buckling, and free vibration of beams and rectangular plates, Comput. Struct. 48 (1993), 473–479.

[37] C. Shu, H. Du, Implementation of clamped and simply supported boundary conditions in the GDQ free vibration analysis of beams and plates, Int. J. Solids Struct. 34 (1997), 819–835.

[38] M. Malik, C. W. Bert, Implementing multiple boundary conditions in the DQ solutıon of hıgher-order PDEs: application to free vibration of plates. Int. J. Numer. Methods Eng. 39(1996), 1237-1258.

[39] W. Dong, Y. Ding, X. Zhu, H. Ding, Differential Quadrature Method for Stability and Sensitivity Analysis of Neutral Delay Differential Systems, J. Dyn. Syst. Measure. Control. 139 (2017) 044504.

[40] Z. Zong, Y. Zhang, Advanced differential quadrature methods, CRC Press, Boca Raton, 2009.

[41] S.S.E. Lam, Application of the differential quadrature method to two-dimensional problems with arbitrary geometry, Comput. Struct. 47 (1993), 459–464.

[42] C.-N. Chen, The development of irregular elements for differential quadrature element method steady-state heat conduction analysis, Comput. Methods Appl. Mech. Eng. 170 (1999), 1–14.

[43] M.M. Chawla, M.A. Al-Zanaidi, An extended trapezoidal formula for the diffusion equation in two space dimensions, Comput. Math. Appl. 42 (2001), 157–168.

[44] M. Tanaka, W. Chen, Coupling dual reciprocity BEM and differential quadrature method for time-dependent diffusion problems, Appl. Math. Model. 25 (2001), 257–268.

[45] F. Wang, Y. Wang, A Coupled Pseudospectral-Differential Quadrature Method for a Class of Hyperbolic Telegraph Equations, Math. Probl. Eng. 2017 (2017), 1–9.

[46] W. Likus, V.A. Vladimirov, Solitary Waves in the Model of Active Media, Taking into Account Effects of Relaxation, Rep. Math. Phys. 75 (2015), 213–230.

[47] V. Volpert, Elliptic Partial Differential Equations Volume 2: Reaction-Diffusion Equations. Basel: Springer, Imprint: Birkhäuser, 2014.

[48] P. Wallisch, ed., MATLAB for neuroscientists: an introduction to scientific computing in MATLAB, Second edition, Academic Press, Amsterdam, 2014.

[49] J.R. Quan, C.T. Chang, New insights in solving distributed system equations by the quadrature method—I. Analysis, Comput. Chem. Eng. 13 (1989), 779–788.

[50] C. Shu, B.E. Richards, High Resolution of Natural Convection in a Square Cavity by Generalized Differential Quadrature. Proceedings of 3rd International Conference on Advances in Numerical Methods in Engineering: Theory and Applications 1990, Swansea, Vol. 2, 978-985.

[51] J.M. Rogers, A.D. McCulloch, A collocation-Galerkin finite element model of cardiac action potential propagation, IEEE Trans. Biomed. Eng. 41 (1994) 743–757.

[52] A.M. Pertsov, J.M. Davidenko, R. Salomonsz, W.T. Baxter, J. Jalife, Spiral waves of excitation underlie reentrant activity in isolated cardiac muscle. Circ. Res. 72 (1993), 631–650.

[53] F.H. Fenton, E.M. Cherry, H.M. Hastings, S.J. Evans, Multiple mechanisms of spiral wave breakup in a model of cardiac electrical activity, Chaos: An Interdisciplinary Journal of Nonlinear Science. 12 (2002), 852–892.

[54] M.L. Steyn-Ross, D.A. Steyn-Ross, L.J. Voss, J.W. Sleigh, Spinodal decomposition in a mean-field model of the cortex: Emergence of hexagonally symmetric activation patterns, Phys. Rev. E. 99 (2019), 012318.